Astron. Astrophys. 330, 1190–1196 (1998)

ASTRONOMY
AND
ASTROPHYSICS

Stability of a slim accretion disk around a black hole

S. Fujimoto and K. Arai

Department of Physics, Kumamoto University, Kumamoto 860, Japan

Received 15 July 1997 / Accepted 14 October 1997

Abstract. Stability is examined for an optically thick, slim accretion disk around a black hole. We derive the fourth-order dispersion relation in a framework of a linear stability analysis. Also we obtain the approximate second-order relation which is convenient to diagnose the stability. By solving these relations for slim disk models with a low viscous parameter α, we find that not only the viscous and thermal modes but the acoustic modes are stabilized at the inner region of the disk when the accretion rate $\dot{M} \geq \dot{M}_{cr} = 16 L_{Edd}/c^2$. On the other hand, when $\dot{M} < \dot{M}_{cr}$, the outward (inward) going acoustic mode is unstable (stable) in the outer region of the disk, though it becomes stable (unstable) at the inner region. The stabilization and destabilization of the acoustic modes are ascribed to such dynamical processes on perturbations as the pressure gradient and advection. Therefore, even if the disk is geometricaly thin ($\dot{M} < \dot{M}_{cr}$), the radial derivatives of physical quantities do play a crucial role for stabilizing the acoustic modes, in contrast to the viscous and thermal modes. The stability of the acoustic modes is very sensitive to the value of α. For models with $\alpha \sim 1$, both the dynamical and thermal effects are important for the stability of the acoustic modes.

Key words: accretion, accretion disks – black hole physics – instability – galaxies: nuclei – X-rays: stars

1. Introduction

It is believed that a black hole exists in some X-ray binaries (Cowley 1992). In such systems, X-ray is probably generated by an accretion disk. Models of an accretion disk around a black hole have been constructed by Shakura & Sunyaev (1973) and Novikov & Thorne (1973) (see also Frank et al. 1992). In these models, it is assumed that the disk is geometrically thin, optically thick and in local thermodynamical equilibrium and gas of the disk rotates in Keplerian circular orbits. Under these assumptions, the basic equations of the flow reduce to a set of algebraic equations. The standard thin disk model can explain observed luminosities and spectra in some X-ray binaries. However, it has been pointed out that physical quantities diverge at the inner edge of the disk (Stoeger 1976). Futhermore, the importance of the radial inertial and pressure gradient terms, which were neglected in the standard model, was stressed by Hoshi & Shibazaki (1977).

As in a case of spherical accretion, an accretion disk around a black hole has transonic nature. The transonic disk accretion has been examined for adiabatic flows by Liang & Thompson (1980), Abramowicz & Zurek (1981), and Loska (1982). Including the radial inertial and pressure gradient terms and taking account of the transonic nature, Matsumoto et al. (1984) have constructed models of a non-adiabatic, thin accretion disk. Abramowicz et al. (1988) have investigated stationary models of *slim accretion disks* with accretion rates comparable to some critical one. They emphasized the significance of the advective cooling for models with supercritical accretion rates and found a characteristically S-shaped curve on the accretion rate versus surface density plane with three branches; the gas pressure dominant *lower* branch, the radiation pressure dominant *middle* branch, and the radiation pressure and advective cooling dominant *upper* branch.

Stability of the standard model has been studied by many authors (Lightman & Eardley 1974, Shibazaki & Hoshi 1975, Shakura & Sunyaev 1976, Pringle 1976). It is found that the radiation pressure dominant thin disk is secularly and thermally unstable. General criteria for the stability of viscous and thermal modes have been derived by Piran (1978). For slim disk models of Abramowicz et al. (1988), thermal runaway is avoided on the *upper* branch due to the advective cooling. This advective stabilization has been recoginized by Abramowicz (1981) and confirmed with the local linear analysis by Wallider (1991) and Chen & Taam (1993) and with the global non-linear analysis by Honma et al. (1991b). Futhermore, Kato et al. (1996,1997) have examined the thermal stability of advection dominated disks against short wavelength perturbations and discussed the effects of the turbulent heat diffusion on the stability.

Kato (1978) suggested a possibility that thin disks are not only viscously and thermally unstable but pulsationally unstable. The cases have been shown by Blumenthal et al. (1984) and Wallinder (1990) where the acoustic modes are pulsationally unstable. Moreover, it has been found that there exist standing

Send offprint requests to: K. Arai

perturbations localized at the transonic point through the pulsational instability (Kato et al. 1988a, b). On the other hand, for slim disk models, Wallinder (1991) has examined the local stability of the acoustic modes and showed that one mode is stable but the other is unstable when $\alpha = 10^{-3}$. Chen & Taam (1993) have also investigated the local stability with a modified prescription of viscosity and found that, when $\alpha = 10^{-1}$ and $\dot{m} = 1$, the outward going acoustic mode is everywhere unstable and the inward going mode is stable in the outer region whereas, in the inner region, it becomes unstable against short wavelength perturbations.

Quasi-periodic oscillations (QPO) are found in some low mass X-ray binaries (e.g. see the review by van der Klis 1989). Particularly, QPO in black hole candidates are thought to be originated from instability of the accretion disk. Concerning models of QPO, the viscous-thermal instability is investigated by Wallinder (1991), Honma et al. (1991a) and Chen & Taam (1994), and the pulsational instability is examined by Blumenthal et al. (1984) and Chen & Taam (1995). Periodic X-ray time variablity of Seyfert galaxy NGC 6841 may be responsible for this instability (Honma et al. 1992, Wallinder 1994).

The aim of the present investigation is to examine the stability of the slim accretion disks in a framework of a linear stability analysis. In particular, we will concentrate our attention on the mechanism for the stabilization of acoustic modes, which has not yet been clearly explained so far.

In Sect. 2 we describe basic equations for a slim accretion disk. A dispersion relation of the fourth order is derived in Sect. 3. Numerical results are presented in Sect. 4. Using an approximate second-order dispersion relation, we diagnose the stability of the acoustic modes. Finally, we summarize our conclusion in Sect. 5.

2. Basic equations

In constructing models of a slim accretion disk around a black hole, we use cylindrical coordinates (r, ϕ, z) centered on the black hole. We assume that the disk is axisymmetric, optically thick, and nonself-gravitating. Futhermore, for simplicity, we take the pseudo-Newtonian potential (Paczyński & Wiita 1980)

$$\Psi = -\frac{GM}{R - r_g}, \tag{1}$$

which simulates quite well general relativistic effects of the Schwarzschild black hole of mass M. Here $R = \sqrt{r^2 + z^2}$ and $r_g = 2GM/c^2$. Using this potential, the Keplerian specific angular momentum l_K of the slim disk is given by

$$l_K = \frac{\sqrt{GMr^3}}{r - r_g}. \tag{2}$$

We assume hydrostatic equilibrium in the z-direction and a polytropic relation between the pressure P and the density ρ for their z-dependence, then we can average hydrodynamic equations of the flow in the vertical direction over the disk thickness $2H$. The vertically integrated pressure W and the surface density Σ are given by

$$W = 2B_1 PH, \quad \Sigma = 2B_2 \rho H,$$

where B_1 and B_2 are the vertically averaging factors expressed as (Hoshi 1977)

$$B_1 = \frac{2^{n+1}(n+1)!}{(2n+3)!!}, \quad B_2 = \frac{2^n n!}{(2n+1)!!}$$

with the polytrope index n.

Since viscosity is the most uncertain in a theory of accretion disks, we adopt the standard α-viscosity (Shakura & Sunyaev 1973) and represent the $r\phi$-component of the viscous stress tensor $\tau_{r\phi}$ as

$$\tau_{r\phi} = -\alpha P. \tag{3}$$

Then the vertically integrated basic equations of the flow become

$$\frac{\partial \Sigma}{\partial t} + \frac{1}{r}\frac{\partial (r\Sigma v_r)}{\partial r} = 0, \tag{4}$$

$$\frac{\partial v_r}{\partial t} + v_r \frac{\partial v_r}{\partial r} + \frac{{l_K}^2 - l^2}{r^3} + \frac{1}{\Sigma}\frac{\partial W}{\partial r} = 0, \tag{5}$$

$$\frac{\partial l}{\partial t} + v_r \frac{\partial l}{\partial r} + \frac{1}{r\Sigma}\frac{\partial (\alpha r^2 W)}{\partial r} = 0, \tag{6}$$

$$\Sigma T \frac{\partial S}{\partial t} = Q^+_{vis} - Q^-_{rad} - Q^-_{adv}. \tag{7}$$

Here v_r is the radial velocity, l is the specific angular momentum, T is the temparature, and S is the specific entropy. Q^+_{vis} is the heating rate per unit disk surface due to viscosity:

$$Q^+_{vis} = \alpha r W \left(-\frac{\partial \Omega}{\partial r}\right), \tag{8}$$

where Ω is the angular velocity. Q^-_{rad} and Q^-_{adv} are the cooling rates per unit disk surface due to radiation and advection, respectively, which are written as

$$Q^-_{rad} = 2B_3 \frac{acT^4}{3\kappa\rho H}, \tag{9}$$

$$Q^-_{adv} = \Sigma v_r T \frac{\partial S}{\partial r}, \tag{10}$$

where a is the radiation density constant, κ is the opacity, and B_3 is the vertically averaging factor given by

$$B_3 = n + 1.$$

The equation of state for a mixture of perfect gas and radiation is

$$P = \frac{k_B \rho T}{\mu m_H} + \frac{1}{3} a T^4,$$

where k_B is the Boltzmann constant, μ the mean molecular weight, and m_H the mass of a hydrogen atom. The opacity is given by the sum of the opacities for the electron scattering κ_{es} and for the free-free absorption κ_{ff}:

$$\kappa = \kappa_{es} + \kappa_{ff}.$$

Throughout the present work, we adopt $\mu = 0.618$ and $n = 3$.

3. Dispersion relation

To examine stability of the steady flow, we perform a linear perturbation analysis for the basic Eqs. (4)–(7) to yield the perturbed Eqs. (A2)–(A5) for

$$u = \frac{\delta\Sigma}{\Sigma}, \quad h = \frac{\delta H}{H}, \quad v = \frac{\delta v_r}{v_r}, \quad j = \frac{\delta l}{l}, \tag{11}$$

where δ represents the Eulerian variation. For a physical quantity, q, of the steady flow, its perturbation is assumed to be expressed in terms of a plane wave

$$\delta q/q \sim \exp[\, i(\omega t - kr)\,], \tag{12}$$

where ω and k are the frequency and wavenumber of the perturbation, respectively. Then Eqs. (A2)–(A5) reduce to four linear algebraic equations

$$C_{i1}u + C_{i2}h + C_{i3}v + C_{i4}j = 0 \quad (i = 1, \ldots, 4).$$

By setting $\det\{C_{ik}\} = 0$, we obtain a fourth-order dispersion relation for $\sigma = i(\omega - kv_r)$. Finally, with use of a dimensionless quantity, $\tilde{\sigma} = \sigma/\Omega_K$, we have

$$C_4\tilde{\sigma}^4 + C_3\tilde{\sigma}^3 + C_2\tilde{\sigma}^2 + C_1\tilde{\sigma} + C_0 = 0. \tag{13}$$

Here, as given by Eqs. (A15)–(A19), the coefficients C_i are functions of physical quantities in steady flow and their radial derivatives.

By solving this dispersion relation, we examine the stability of the steady flow. When $Re(\sigma)$ is less (greater) than zero, the steady flow is stable (unstable) against the perturbation. If $Im(\sigma)$ is negative (positive), the perturbation is an inward (outward) going wave.

4. Results and discussion

A sequence of stationary models is constructed from numerical integrations of Eqs. (4)–(7) with the suitable boundary conditions. Our models contain three parameters, M, $\dot{m}$ and α. Here

$$\dot{m} = \dot{M}/\dot{M}_{cr}, \tag{14}$$

where $\dot{M}$ is the mass accretion rate and $\dot{M}_{cr}$ is the critical rate given by

$$\dot{M}_{cr} = \frac{16L_{Edd}}{c^2} \tag{15}$$

with the Eddington luminosity L_{Edd}.

We consider the models with $0.1 \le \dot{m} \le 10$, $M = 10M_\odot$ and $\alpha = 10^{-3}$, but the dependence of stability on M and α will be discussed at the end of this section. We have obtained qualitatively the same stationary models as given by Abramowicz et al. (1988), Arai & Iimori (1992), and Chen & Taam (1993).

Now we solve the fourth-order dispersion relation (13) for the steady flows. There exist four roots which correspond to one viscous, one thermal, and two acoustic modes. We find that the roots are larger for the acoustic modes than those for the viscous and thermal modes when α is small. Moreover, our results agree quite well with those of Wallinder (1991) for the viscous and thermal modes. We, therefore, concentrate our interests on the acoustic modes.

If $\alpha \ll 1$, the terms of the order α^2 and higher can be neglected. Then Eq. (13) reduces to

$$\begin{aligned} E_h\tilde{\sigma}^2 &+ [\,(d_l + 2d_v)\tilde{v}_r E_h - S_h + \tilde{v}_r D_h\,]\tilde{\sigma} \\ &+ \tilde{\chi}^2 E_h + \tilde{c}_s^2\xi^2(E_h - 2E_u) + 2\tilde{c}_s^2 d_W D_v \\ &+ 2i\tilde{c}_s^2\xi(D_v - d_W E_u) = 0. \end{aligned} \tag{16}$$

Here $\xi = kr$, $d_q = d\ln|q|/d\ln r$, $\tilde{v}_r = v_r/v_K$, $\tilde{\chi} = \chi/\Omega_K$, and $\tilde{c}_s = c_s/v_K$, where $\chi = \sqrt{2d_l}\Omega$ is the epicyclic frequency and $c_s = \sqrt{W/\Sigma}$ is the sound velocity. E_u, E_h, S_h, D_h and D_v are given by Eqs. (A7), (A8), (A10), (A12) and (A13), respectively. We note that, in the standard model where $d_q = 0$, the stability of the viscous and thermal modes is determined from the sign of S_h; if $S_h < 0$ then these modes are stable; otherwise they are unstable. The approximate second-order dispersion relation (16) is useful for diagnosing the stability of the acoustic modes.

Fig. 1 shows the growth rates of the acoustic modes as a function of $\lambda = 2\pi/k$ for models with $\dot{m} = 0.1$ and 10. The solid lines denote the solutions to the fourth-order dispersion relation (13) and the dotted lines are to the second-order dispersion relation (16). We can see that both solutions agree with each other and $|Re(\tilde{\sigma})|$ tends to decrease as λ increases. It can be seen from panel (a) that the acoustic mode is stabilized at $r = 5\,r_g$ when $\lambda \ge 15H$ and $\dot{m} = 10$.

Fig. 2 shows $Re(\tilde{\sigma})$ as a function of $\dot{m}$ for the perturbations with $\lambda/H = 5$ and 20. Except when $\dot{m} \ge 1$ at $r = 5\,r_g$, $Re(\tilde{\sigma})$ has the same magnitudes but the opposite signs as is obtained by Wallinder (1991).

We find that the third and fourth terms are the most dominant in Eq. (16). Therefore we obtain

$$Im(\tilde{\sigma}) \simeq \pm\sqrt{\tilde{\chi}^2 + \tilde{c}_s^2\xi^2\left(1 - 2\frac{E_u}{E_h}\right)}, \tag{17}$$

$$Re(\tilde{\sigma}) \simeq \mp G_1 + G_2 - G_3, \tag{18}$$

where

$$G_1 = \frac{\tilde{c}_s^2\xi}{E_h|Im(\tilde{\sigma})|}(D_v - d_W E_u), \tag{19}$$

$$G_2 = \frac{S_h}{2E_h}, \tag{20}$$

$$G_3 = \frac{1}{2}\left(d_l + 2d_v + \frac{D_h}{E_h}\right)\tilde{v}_r. \tag{21}$$

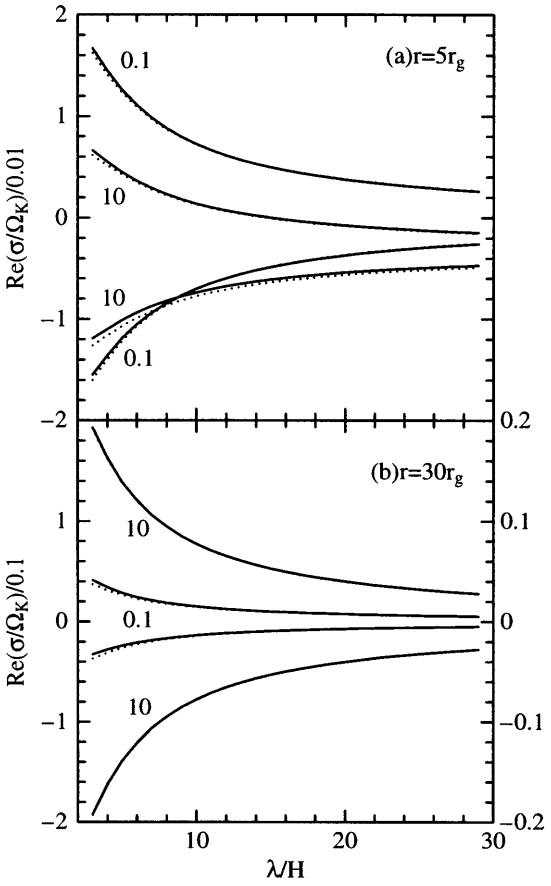

Fig. 1a and b. Growth rates of the perturbations with the wavelength λ for models with $\dot{m}$ = 0.1 and 10. The solid lines and dotted lines denote the solutions to the fourth-order dispersion relation (13) and the second-order one (16), respectively. **a** corresponds to a radius of $5\,r_g$, while **b** corresponds to a radius of $30\,r_g$, where the scale of the vertical axis for $\dot{m}$ = 10 is ten times that for $\dot{m}$ = 0.1.

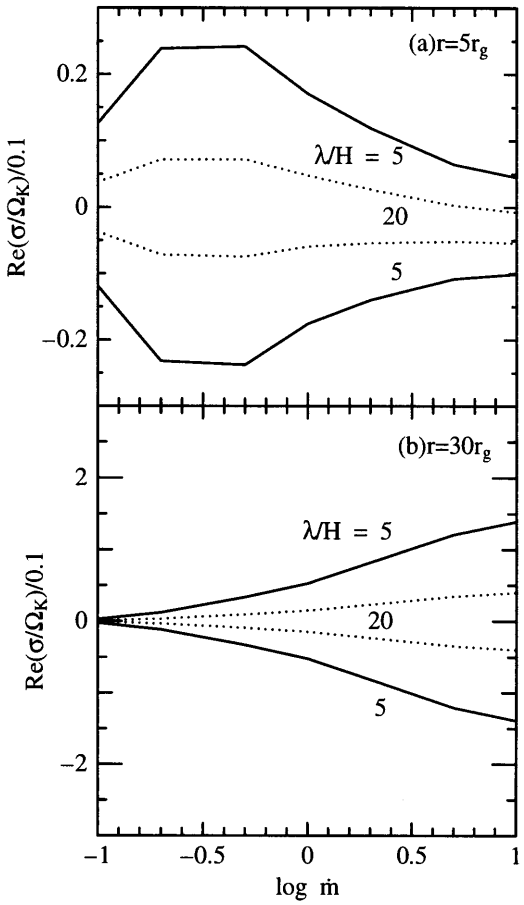

Fig. 2. The variation of the growth rates with respect to the accretion rate for the acoustic modes when $\lambda = 5H$ (solid lines) and $\lambda = 20H$ (dashed lines).

We show in Fig. 3a the magnitude of each term in the right-hand side of Eq. (18) for a model with $\dot{m}$ = 0.1 and $\lambda = 20H$. The solid line, which represents the first term G_1, has an apparent dip at $r \sim 8\,r_g$. This is due to the fact that temparature and pressure are maximum and consequently the radial derivatives D_v and d_W change their signs at that point. The dotted line is also not smooth at $r \sim 32\,r_g$ because S_h changes its sign. From Fig. 3a, except at $r \sim 8\,r_g$, we can see

$$|G_1| \gg |G_2| \gg |G_3|. \tag{22}$$

Hence we obtain

$$Re(\tilde{\sigma}) \simeq \mp G_1. \tag{23}$$

Eventually, $Re(\tilde{\sigma})$ has the same magnitudes with the opposite signs. Since $E_u < 0$ and $E_h > 0$, at the outer region of the disk, where $D_v < 0$ and $d_W < 0$, the outward (inward) going mode is unstable (stable). On the other hand, at the inner region, where $D_v > 0$ and $d_W > 0$, the outward (inward) going mode is stable (unstable). Thus, even if $\dot{m} < 1$, the advective cooling and the radial derivatives play a crucial role for stabilizing the acoustic modes, in contrast to the viscous and thermal modes. It should be noted that the approximate solution (23) can be derived from a dispersion relation for an inviscid, adiabatic perturbation. This is because, when α is small, the angular momentum loss and viscous heating have only minor effects on the perturbations.

Fig. 3b shows the magnitudes of G_1, G_2 and G_3 for a model with $\dot{m}$ = 10, where the same apparent dip appears at $r \sim 6\,r_g$ in the solid line as in Fig. 3a. Since G_1 is the most dominant at $r > 10\,r_g$, $Re(\tilde{\sigma})$ is given by Eq. (23) as in the case of $\dot{m}$ = 0.1. On the other hand, at $r < 10\,r_g$, instead of the inequality (22) we obtain the following relation

$$|G_1| \sim |G_3| > |G_2|. \tag{24}$$

Therefore, two acoustic modes are stabilized at the inner region because the radial drift term G_3 is positive. The stabilization sets in when G_3 becomes significantly important. As ξ decreases with increasing wavelength, the magnitude of G_1 decreases. Then, as can be seen from Fig. 2a, the acoustic modes tend to be stabilized for long wavelength perturbations.

Finally we discuss how the stability depends on the parameters α and M. Because d_q is weakly dependent on both α and

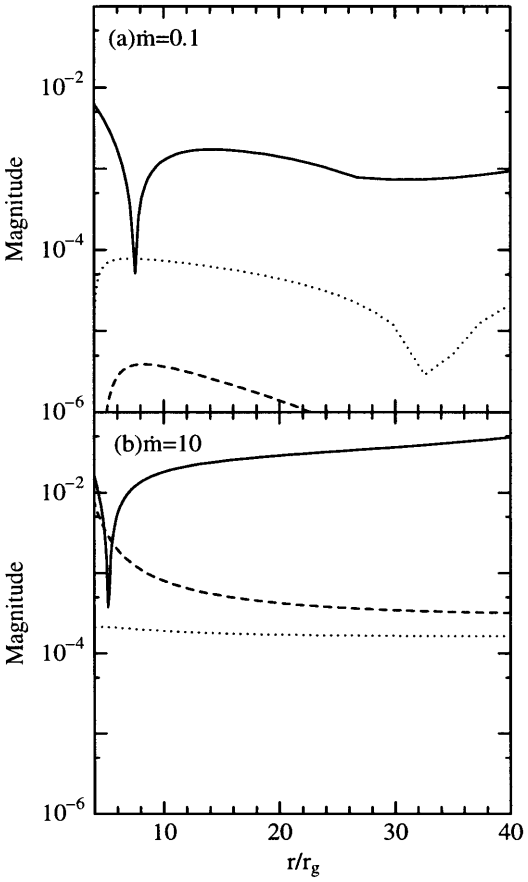

Fig. 3. Magnitude of each term of the right-hand side of Eq. (18) as a function of the radius for $\dot{m} = 0.1$ and 10 when $\lambda = 20H$. The solid, dotted, and dashed lines represent the terms G_1, G_2 and G_3, respectively.

M for a radiation pressure dominant disk, the terms (19) – (21) vary as

$$G_1 \propto \dot{m}, \quad G_2 \propto \alpha, \quad G_3 \propto \alpha\dot{m}^2. \tag{25}$$

Note that M does not appear in the above expressions. Therefore, we can see that the stability of the acoustic modes is insensitive to M. It is, however, strongly dependent on α. When $\alpha < 10^{-3}$, the second and third terms in Eq. (18) can be neglected, being compared with the first term even if $\dot{m} \geq 1$. Therefore, one mode is stable while the other is unstable. As α increases, the relative importance of the second and third terms increases. Accordingly, the acoustic modes tend to be stabilized through the dynamical processes at the inner region just as discussed above (see Fig. 3). If α increases further and the second term is comparable to the first term, the thermal effects may contribute to the stability of the acoustic modes as well as the dynamical effects. However, the approximation of Eq. (16) is no more valid when $\alpha \sim 1$.

5. Conclusions

We have constructed stationary models of a slim accretion disk around a black hole and examined stability of the steady flows in a framework of a linear perturbation analysis. By solving the fourth-order and the approximate second-order dispersion relations, the following conclusions have been obtained for the acoustic modes: (a) In the case of $\alpha \ll 1$ and $\dot{m} < 1$, the outward (inward) going mode is unstable (stable) at the outer region of the disk, while it is stable (unstable) at the inner region. (b) The growth rates of the perturbations are determined from such dynamical processes as the pressure gradient and advection. The radial derivatives of vertically integrated pressure and entropy are particularly important. (c) For disk models with $\dot{m} \geq 1$, the outward and inward modes are stabilized because of the existence of the radial drift term G_3. (d) The radial derivatives of physical quantities do play a crucial role for stabilizing the acoustic modes. (e) The stability of the acoustic modes is insensitive to M. (f) When $\alpha \sim 1$, both dynamical and viscous non-adiabatic processes are important for the stability.

In the present paper, we have considered only viscous dissipation as a heating source. However, energy produced through hydrogen burning deep inside the disk is comparable to energy generated by the dissipation when α becomes as low as 10^{-5} (Arai & Hasimoto, 1995). It is worthwhile to examine the stability of a slim accretion disk with nuclear burning.

Recently, optically thin, advection dominated disk models have received much attention (Narayan & Yi 1995, Narayan 1996). It is shown by Manmoto et al. (1996) that the disks are thermally unstable against short wavelength perturbations. Wu & Li (1996) have studied the local stability of such models, but neglected radial derivatives of physical quantities in deriving the dispersion relation. These derivatives are important for the stability of the optically thick disk as stressed in the present investigation. We need further studies to confirm the importance of the derivatives in these models.

Appendix A: derivation of a dispersion relation

We present detailed derivation of the fourth-order dispersion relation (13). Let us introduce dimensionless quantities as

$$u = \frac{\delta\Sigma}{\Sigma}, \quad h = \frac{\delta H}{H}, \quad v = \frac{\delta v_r}{v_r}, \quad j = \frac{\delta l}{l}. \tag{A1}$$

In a framework of a linear stability analysis, the hydrodynamical Eqs. (4)–(7) yield the perturbed equations

$$\tilde{D}_t u + \tilde{v}_r \frac{\partial}{\partial \ln r} v = 0, \tag{A2}$$

$$\tilde{c}_s \frac{\partial}{\partial \ln r} u + 2\tilde{c}_s \left(d_W + \frac{\partial}{\partial \ln r} \right) h + \tilde{v}_r \left(\tilde{D}_t + 2\tilde{v}_r d_v \right) v - 2\tilde{l}^2 j = 0, \tag{A3}$$

$$\frac{1}{d_W + 2} \frac{\partial}{\partial \ln r} u - 2\left(1 + \frac{1}{d_W + 2} \frac{\partial}{\partial \ln r} \right) h$$

$$+ v + \left(1 + \frac{\tilde{D}_t}{d_l \tilde{v}_r}\right) j = 0, \tag{A4}$$

$$(E_u \tilde{D}_t - S_u + \tilde{v}_r D_u)u + (E_h \tilde{D}_t - S_h + \tilde{v}_r D_h)h + (\tilde{v}_r D_v)v - B_4 W_{vis}\left(1 + \frac{1}{d_\Omega}\frac{\partial}{\partial \ln r}\right) j = 0. \tag{A5}$$

Here

$$\tilde{v}_r = v_r/v_K, \quad \tilde{c}_s = c_s/v_K, \quad \tilde{l} = l/l_K,$$

$$\tilde{D}_t = \frac{1}{\Omega_K}\frac{\partial}{\partial t} + \tilde{v}_r \frac{\partial}{\partial \ln r}, \tag{A6}$$

$$d_q = \frac{d \ln |q|}{d \ln r},$$

$$E_u = \frac{-8 + 3\beta + 3\beta^2}{2(4 - 3\beta)}, \tag{A7}$$

$$E_h = \frac{56 - 45\beta - 3\beta^2}{2(4 - 3\beta)}, \tag{A8}$$

where β is the ratio of gas to total pressure.

$$S_u = \frac{B_4}{W\Omega_K}\left[\left(\frac{\partial Q^+_{vis}}{\partial \ln \Sigma}\right)_H - \left(\frac{\partial Q^-_{rad}}{\partial \ln \Sigma}\right)_H\right] = B_4\left(W_{vis} + W_{rad}\frac{\beta + a_{ff}(1+\beta)}{4 - 3\beta}\right), \tag{A9}$$

$$S_h = \frac{B_4}{W\Omega_K}\left[\left(\frac{\partial Q^+_{vis}}{\partial \ln H}\right)_\Sigma - \left(\frac{\partial Q^-_{rad}}{\partial \ln H}\right)_\Sigma\right] = B_4\left(2W_{vis} - W_{rad}\frac{8(1+\beta) + a_{ff}(15+\beta)}{2(4-3\beta)}\right), \tag{A10}$$

where $W_{vis} = Q^+_{vis}/(W\Omega_K)$, $W_{rad} = Q^-_{rad}/(W\Omega_K)$, $a_{ff} = \kappa_{ff}/\kappa$, and $B_4 = B_1/B_2$.

$$D_u = F_1(1 - F_2)(d_{F_1} + d_W - d_\Sigma) - F_1 F_2 d_{F_2} - d_\rho, \tag{A11}$$

$$D_h = F_1(2 + 7F_2)(d_{F_1} + d_W - d_\Sigma) + 7F_1F_2 d_{F_2} - 2d_\rho, \tag{A12}$$

$$D_v = \frac{3}{2}(8 - 7\beta)d_T - (4 - 3\beta)d_\rho, \tag{A13}$$

where $F_1 = 3(1 - \beta/2)$ and $F_2 = \beta(1-\beta)/[(2-\beta)(4-3\beta)]$.

If the perturbation is expressed as $\delta q/q \sim \exp[\, i(\omega t - kr)\,]$, then Eqs. (A2)–(A5) reduce to four linear algebraic equations

$$C_{i1}u + C_{i2}h + C_{i3}v + C_{i4}j = 0 \quad (i = 1, \ldots, 4).$$

Using a dimensionless quantity $\tilde{\sigma} = i(\omega - kv_r)/\Omega_K$ and setting $\det\{C_{ik}\} = 0$, we obtain a fourth-order dispersion relation

$$C_4\tilde{\sigma}^4 + C_3\tilde{\sigma}^3 + C_2\tilde{\sigma}^2 + C_1\tilde{\sigma} + C_0 = 0. \tag{A14}$$

Here C_i are given by

$$C_4 = E_h, \tag{A15}$$

$$C_3 = (d_l + 2d_v)v_r E_h - A_2, \tag{A16}$$

$$C_2 = -(d_l + 2d_v)v_r A_2 + (\chi^2 + c_s^2\xi^2 + 2v_r^2 d_v d_l)E_h - 2c_s^2\xi^2 E_u - 2c_s^2 d_W D_v + 2B_4\alpha(v_r l d_l d_\Omega + \alpha c_s^2\xi^2) + 2i\xi[\, c_s^2(D_v - d_W E_u) + B_4\alpha(\alpha c_s^2 d_\Omega - v_r l d_l)\,], \tag{A17}$$

$$C_1 = 2c_s^2\xi^2 A_1 - (\chi^2 + c_s^2\xi^2 + 2v_r^2 d_v d_l)A_2 + c_s^2\xi^2(v_r d_l + 2\alpha l)(E_h - 2E_u) + 2(\chi^2 - c_s^2 d_l d_W)v_r D_v + 2B_4\alpha[\, c_s^2 l d_l(d_W d_\Omega - \xi^2) + 2v_r d_v(v_r l d_l d_\Omega + \alpha c_s^2\xi^2)\,] + 2i\xi[\, c_s^2 d_W A_1 + (\chi^2 - c_s^2 d_l d_W)v_r E_u + c_s^2(v_r d_l + 2\alpha l)D_v - B_4\alpha c_s^2 l d_l(d_W + d_\Omega) + 2B_4\alpha v_r d_v(\alpha c_s^2 d_\Omega - v_r l d_l)\,], \tag{A18}$$

$$C_0 = c_s^2\xi^2[\,(v_r d_l + 2\alpha l)(2A_1 - A_2) + 2B_4\alpha d_\Omega(\alpha c_s^2 d_W + v_r l d_l)\,] - 2i\xi[\,(\chi^2 - c_s^2 d_l d_W)v_r A_1 + B_4\alpha c_s^2\xi^2(\alpha c_s^2 d_W + v_r l d_l)\,], \tag{A19}$$

where

$$\xi = kr, \quad \chi = \sqrt{2d_l}\,\Omega/\Omega_K,$$

$$A_1 = S_u - v_r D_u,$$

$$A_2 = S_h - v_r D_h.$$

Note that in the expressions for C_i and A_i, we omit, for simplicity, the simbol tilde.

References

Abramowicz M.A., 1981, Nat 294, 235
Abramowicz M.A., Czerny B., Lasota J.P., Szuszkiewicz E., 1988, ApJ 332, 646
Abramowicz M.A., Zurek W.H., 1981, ApJ 246, 314
Arai K., Hashimoto M., 1995, A&A 302, 99
Arai K., Iimori T., 1992, Phys. Rep. Kumamoto Univ. 9, 51
Blumenthal G.R., Yang L.T., Lin D.N.C., 1984, ApJ 287, 774
Chen X., Taam R.E., 1993, ApJ 412, 254
Chen X., Taam R.E., 1994, ApJ 431, 732
Chen X., Taam R.E., 1995, ApJ 441, 354
Cowley A.P., 1992, ARA&A 30, 287
Frank J., King A.R., Raine D.J., 1992, *Accretion Power in Astrophysics*, 2nd ed., Cambridge Univ. Press, Cambridge
Honma F., Matsumoto R., Kato S., 1991a, PASJ 43, 147
Honma F., Matsumoto R., Kato S., 1992, PASJ 44, 529
Honma F., Matsumoto R., Kato S., Abramowicz M.A., 1991b, PASJ 43, 261
Hoshi R., 1977, Prog. Theor. Phys. 58, 1191
Hoshi R., Shibazaki N., 1977, Prog. Theor. Phys. 58, 1759

Kato S., 1978, MNRAS 185, 629
Kato S., Abramowicz M., Chen X., 1996, PASJ 48, 67
Kato S., Honma F., Matsumoto R., 1988a, MNRAS 231, 37
Kato S., Honma F., Matsumoto R., 1988b, PASJ 40, 709
Kato S., Yamasaki T., Abramowicz M., Chen X., 1997, PASJ 49, 221
Liang E.P.T., Thompson K.A., 1980, ApJ 240, 271
Lightman A.P., Eardley D.M., 1974, ApJ 187, L1
Loska Z., 1982, Acta Astr. 32, 13
Manmoto T., et al. 1996, ApJ 464 L135
Matsumoto R., Kato S., Fukue J., Okazaki A.T., 1984, PASJ 36, 71
Narayan R., Yi I., 1995, ApJ 452, 710
Narayan R., 1996, in *Physics of Accretion Disk* eds. S. Kato et al. Gordon and Breach, Amsterdam, p. 15
Novikov I.D., Thorne K.S., 1973, in *Black Holes* eds. B. DeWitt, C.DeWitt, Gordon and Breach, New York, p. 343
Pringle J.E., 1976, MNRAS 177, 65
Paczyński B., Wiita P.J., 1980, A&A 88, 23
Piran T., 1978, ApJ 221, 652
Shakura N.I., Sunyaev R.A., 1973, A&A 24, 337
Shakura N.I., Sunyaev R.A., 1976, MNRAS 175, 613
Shibazaki N., Hoshi R., 1975, Prog. Theor. Phys. 54, 706
Stoeger W.R., 1976, A&A 53, 267
van der Klis M., 1989, ARA&A 27, 517
Wallinder F.H., 1990, A&A 237, 207
Wallinder F.H., 1991, A&A 249, 107
Wallinder F.H., 1994, in *Theory of Accretion Disks - 2*, eds. W.J. Duschl et al., Kluwer Academic Pub., Dordrecht, p. 287
Wu X.B., Li Q.B., 1996, ApJ 469, 776

This article was processed by the author using Springer-Verlag LaTeX A&A style file *L-AA* version 3.